Spin labeling of the Escherichia coli NADH ubiquinone oxidoreductase (complex I). Biochim Biophys Acta

ARTICLE *in* BIOCHIMICA ET BIOPHYSICA ACTA · OCTOBER 2010

Impact Factor: 4.66 · DOI: 10.1016/j.bbabio.2010.10.013 · Source: PubMed

11 AUTHORS, INCLUDING:

Muege Aksoyoglu
University of Freiburg
2 PUBLICATIONS **178** CITATIONS
SEE PROFILE

Erik Schleicher
University of Freiburg
57 PUBLICATIONS **1,742** CITATIONS
SEE PROFILE

Arpad Rostas
University of Freiburg
0 PUBLICATIONS **0** CITATIONS
SEE PROFILE

Corinne Boudon
University of Strasbourg
164 PUBLICATIONS **3,700** CITATIONS
SEE PROFILE

Biochimica et Biophysica Acta 1797 (2010) 1894–1900

Contents lists available at ScienceDirect

Biochimica et Biophysica Acta

journal homepage: www.elsevier.com/locate/bbabio

Spin labeling of the *Escherichia coli* NADH ubiquinone oxidoreductase (complex I)

Thomas Pohl [a,1], Thomas Spatzal [a,1], Müge Aksoyoglu [b], Erik Schleicher [b], Arpad Mihai Rostas [b], Helga Lay [a], Udo Glessner [a], Corinne Boudon [c], Petra Hellwig [d], Stefan Weber [b], Thorsten Friedrich [a,*]

[a] Institut für Organische Chemie und Biochemie, Albert-Ludwigs-Universität Freiburg, Albertstr. 21, 79104 Freiburg, Germany
[b] Institut für Physikalische Chemie, Albert-Ludwigs-Universität Freiburg, Albertstr. 21, 79104 Freiburg, Germany
[c] Laboratoire d'electrochimie et chimie physique du corps solide, Institut de Chimie UMR 7177, CRNS - Université de Strasbourg, 4, rue Blaise Pascal, 67070 Strasbourg, France
[d] Institut de Chimie UMR 7177, Laboratoire de spectroscopie vib. et electrochimie des biomolecules, CNRS - Université de Strasbourg, 1, rue Blaise Pascal, 67070 Strasbourg, France

ARTICLE INFO

Article history:
Received 31 October 2009
Received in revised form 29 September 2010
Accepted 13 October 2010
Available online 16 October 2010

Keywords:
Complex I
NADH:ubiquinone oxidoreductase
Quinone binding site
Spin labeling
EPR spectroscopy
Escherichia coli

ABSTRACT

The proton-pumping NADH:ubiquinone oxidoreductase, the respiratory complex I, couples the transfer of electrons from NADH to ubiquinone with the translocation of protons across the membrane. Electron microscopy revealed the two-part structure of the complex with a peripheral arm involved in electron transfer and a membrane arm most likely involved in proton translocation. It was proposed that the quinone binding site is located at the joint of the two arms. Most likely, proton translocation in the membrane arm is enabled by the energy of the electron transfer reaction in the peripheral arm transmitted by conformational changes. For the detection of the conformational changes and the localization of the quinone binding site, we set up a combination of site-directed spin labeling and EPR spectroscopy. Cysteine residues were introduced to the surface of the *Escherichia coli* complex I. The spin label (1-oxyl-2,2,5,5-tetramethyl-Δ3-pyrroline-3-methyl)-methanethiosulfonate (MTSL) was exclusively bound to the engineered positions. Neither the mutation nor the labeling had an effect on the NADH:decyl-ubiquinone oxidoreductase activity. The characteristic signals of the spin label were detected by EPR spectroscopy, which did not change by reducing the preparation with NADH. A decyl-ubiquinone derivative with the spin label covalently attached to the alkyl chain was synthesized in order to localize the quinone binding site. The distance between a MTSL labeled complex I variant and the bound quinone was determined by continuous-wave (cw) EPR allowing an inference on the location of the quinone binding site. The distances between the labeled quinone and other complex I variants will be determined in future experiments to receive further geometry information by triangulation.

1. Introduction

The proton-pumping NADH:ubiquinone oxidoreductase, the respiratory complex I, couples the electron transfer from NADH to ubiquinone with the translocation of protons across the membrane [1–5]. The bacterial complex I is a minimal structural form of an energy-converting NADH:ubiquinone oxidoreductase and consists in general of 14 different subunits [6–9]. In *Escherichia coli* and a few other bacteria, the genes *nuoC* and *nuoD* are fused resulting in a complex that consists of 13 subunits called NuoA-N with a total molecular mass of 535 kDa [10,11]. Electron microscopy revealed that the complex is built of a peripheral arm and a membrane arm [12–16]. Six or seven subunits, respectively, constitute the peripheral arm containing all known redox groups, namely 1 flavin mononucleotide (FMN) and up to 10 iron-sulfur clusters [17,18] as well as the NADH binding site. The membrane arm consists of seven highly hydrophobic subunits comprising 61 transmembrane helices [5,15]. So far, no cofactors have been detected in the arm. However, it must be involved in proton translocation as it represents the only membrane-spanning part of the complex. So far, the ubiquinone binding site has not been unambigously localized. From analyses of mutants resistant to inhibitors of the quinone binding site, it has been concluded that the site is located between the peripheral arm and the membrane arm [19,20]. However, there is no direct evidence on a molecular level that the inhibitor binding site is identical with the quinone binding site.

It is discussed that the proton translocation is induced by conformational changes [2,4,6,21,22]. Although it is widely accepted that the reaction of complex I is associated with conformational changes [21–26], it is not clear whether they play a role in proton translocation.

Here, we introduce site-directed spin labeling (SDSL) of complex I in combination with EPR spectroscopy [27] as a method of detecting the dynamics of complex I and localizing the ubiquinone binding site on a molecular level. In this approach, a spin label is attached to distinct positions of the protein and its signal characterized by means of EPR spectroscopy. The most frequently used spin label is (1-oxyl-2,2,5,5,-tetramethyl-Δ3-pyrolline-3-methyl)-methanethiosulfonate (MTSL) [28] which can be covalently attached to cysteine residues on the protein surface. The shape of the EPR spectrum of the label is dominated

* Corresponding author. Tel.: +49 761 203 6060; fax: +49 761 203 6096.
E-mail address: Thorsten.Friedrich@uni-freiburg.de (T. Friedrich).
[1] These authors contributed equally to this study.

0005-2728/$ – see front matter © 2010 Elsevier B.V. All rights reserved.
doi:10.1016/j.bbabio.2010.10.013

by its mobility, which depends on the local protein structure, and is mainly influenced by tertiary interactions with neighboring secondary structure elements. Thus, SDSL is used to probe the local protein structure and to pinpoint structural changes [29–32].

A quantitative interpretation of the spectral changes is not possible only by means of SDSL, because changes in the label mobility are not proportional to the amplitude of local structural changes [33]. To solve this problem, two spin labels can be introduced, thus allowing distance measurements in a so-called double site-directed spin labeling experiment [34]. The method is based on the measurement of the strength of dipolar interactions between two spin labels [35], which is inversely proportional to the cubed distance [36,37], and thus is used to determine distances. Here, we describe a method of localizing the ubiquinone binding site of complex I by introducing a novel spin labeled decyl-ubiquinone (Q_{10}-MTSL) to measure distances between distinct positions of complex I and the Q_{10}-MTSL.

2. Generation of surface cysteine variants and MTSL labeling

A prerequisite for SDSL studies is the pinpoint introduction of cysteine residues into regions of interest. In addition, unspecific label binding to the protein surface has to be excluded. We used the episomal expression system recently developed in our group to produce site-directed variants of the *E. coli* complex I, which were purified by means of affinity chromatography [38]. Mutations were introduced by Lambda-Red mediated recombineering as described previously [38] and verified by sequencing. Positions for the introduction of cysteine residues were selected from the crystal structure of the peripheral arm of *Thermus thermophilus* complex I [39]. The selected residues were neither conserved nor did they show any obvious structural function (Fig. 1). So far, we have created six cysteine variants of complex I with mutations close to the NADH binding site ($E156C^{NuoE}$ and $D56C^{NuoF}$) at positions in the middle of the peripheral arm ($E84C^{NuoG}$ and $E298C^{NuoG}$) and close to the proposed quinone binding site ($R112C^{NuoB}$). In addition, a position within a loop region of the hydrophobic subunit NuoM of the membrane arm ($T166C^{NuoM}$) was chosen by calculating the subunit topology according to the majority vote approach [40]. The positions are numbered according to the *E. coli* amino acid sequence (Fig. 1).

To ensure that the selected positions were accessible to the spin label and to demonstrate that the wild type complex was not labeled, the isolated complex I and its variants were incubated with the

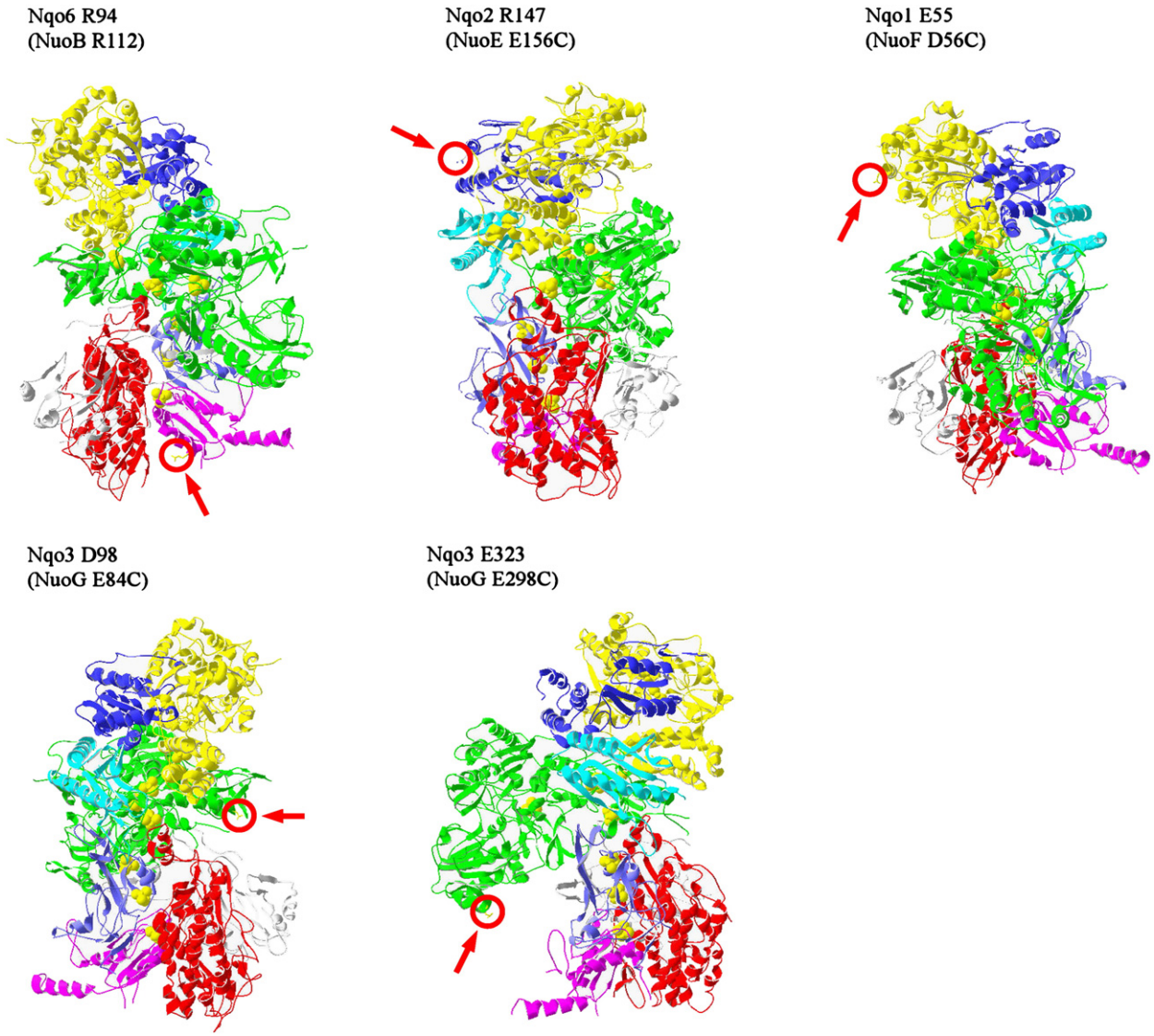

Fig. 1. Positions of selected surface amino acids that were exchanged to cysteine residues and labeled with MTSL. The structure of the peripheral arm of the *T. thermophilus* complex I is used (PDB ID: 2FUG, Sazanov and Hinchliffe [39]). The subunits are shown in different colors. The position of individual amino acids is given in the *T. thermophilus* and *E. coli* (in brackets) nomenclature as derived from sequence comparisons. The positions exchanged to cysteine residues are marked with red circles. For a better representation, different views of the protein are shown.

fluorescent dye tetramethylrhodamine (TMR)-maleimide exhibiting the same reactivity as MTSL. The samples were subjected to SDS-PAGE (Fig. 2). The lanes stained with Coomassie brilliant blue showed the presence of all complex I subunits, and the inverted fluorograms of the unstained gels demonstrated that TMR-maleimide was only attached to the subunits carrying the engineered cysteine residue. The presence of minor bands containing less than 10% of the bound label was either due to a proteolytic digestion of the labeled subunit (labeling of NuoG) or due to minor impurities (labeling of NuoB, E, and F) as determined by mass spectrometric analyses. The wild type complex I was not labeled by TMR-maleimide (data not shown). Labeling with MTSL prior to the incubation with TMR prevented binding of the fluorophor (Fig. 2) indicating that MTSL bound and blocked the corresponding positions. Thus, the variants were selectively labeled with MTSL at the desired positions.

Table 1
NADH:decyl-ubiquinone oxidoreductase activity of various complex I variants reconstituted in *E. coli* polar lipids (Avanti) before and after labeling with MTSL (Toronto Research Chemicals Inc.). The slightly higher activities obtained after labeling are due to the additional purification step to remove the excess label.

Variant	NADH:decyl-ubiquinone oxidoreductase activity [μmol min^{-1} mg^{-1}]	
	Before incubation with MTSL	After incubation with MTSL
Native	3.2	3.3
$R112C^{NuoB}$	2.1	2.3
$E156C^{NuoE}$	1.4	1.6
$D56C^{NuoF}$	3.1	3.3
$E84C^{NuoG}$	2.6	3.2
$E298C^{NuoG}$	2.5	2.6
$T166C^{NuoM}$	2.7	3.0

3. Influence of spin labeling on the enzymatic activity

To determine a possible influence of the mutations and the MTSL labeling on the functionality of complex I, the NADH:decyl-ubiquinone oxidoreductase activity of the variants before and after labeling was determined. For the assay, the isolated complex I variants were reconstituted in *E. coli* polar lipids [41]. The enzymatic activity of an aliquot was determined. Another aliquot was incubated with MTSL, the excess label was removed by gelfiltration and the activity determined (Table 1). The data demonstrate that neither mutation nor labeling had an effect on the physiological activity of complex I. Thus, SDSL is potentially well suited for the study of the *E. coli* complex I.

4. EPR spectra of MTSL covalently attached to complex I

For EPR spectroscopic characterization, the wild type and its variants were incubated with MTSL, the excess label removed by gelfiltration, and the proteins reconstituted into lipids as described previously [41]. Spectra were recorded at room temperature using X-band EPR. The wild type complex showed no signal (Fig. 3), again demonstrating that no spin label was attached. The free MTSL showed the typical isotropic spectrum with three lines resulting from hyperfine interaction of the unpaired electron spin with the nitrogen nuclear spin (Fig. 3). The mobility of the MTSL was restricted due its covalent attachment to the protein. As a consequence, the signals of the label bound to the complex I variants exhibited broader central resonance lines, broader outer lines, and a subtle increase in the hyperfine splitting reflecting the confined mobility of the label (Fig. 3).

The EPR signals were analyzed in terms of empirical parameters, namely the inverse linewidth of the central resonance line (ΔH_0^{-1}) and the distance of the outer hyperfine extrema ($2A_{ZZ}$) as indicated in Fig. 3 [29,41]. In general, a broad central resonance line and a great distance to the outer hyperfine extrema reflect the label's restricted motion [33]. The mobility of the label is influenced by (i) the rotational correlation time τ_R of the protein, (ii) the effective correlation time τ_B due to the rotation of the label around the linker bonds between the MTSL and the protein backbone, and (iii) the effective correlation time τ_S due to the

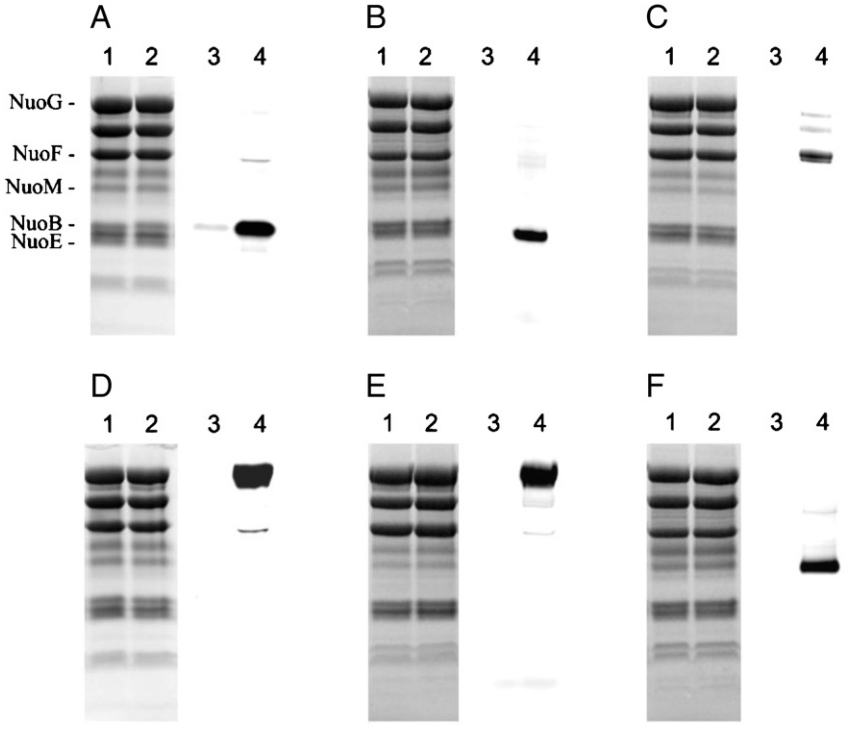

Fig. 2. Identification of covalently labeled subunits of various complex I variants. The samples were incubated with 1.2 molar equivalents of TMR-maleimide for 20 min on ice either before (lanes 2 and 4) or after coupling with MTSL (lanes 1 and 3). The subunit pattern of the variant (A) $R112C^{NuoB}$, (B) $E156C^{NuoE}$, (C) $D56C^{NuoF}$, (D) $E84C^{NuoG}$, (E) $E298C^{NuoG}$, and (F) $T166C^{NuoM}$ is shown. The position of some complex I subunits are marked in (A) for a better assignment. Each lane was loaded with 75 μg complex I. Lanes 1 and 2 were stained with Coomassie-brilliant blue, lanes 3 and 4 show the inverted fluorogramms. The reaction was stopped by an addition of DTT and loaded on a 10% SDS-PAGE.

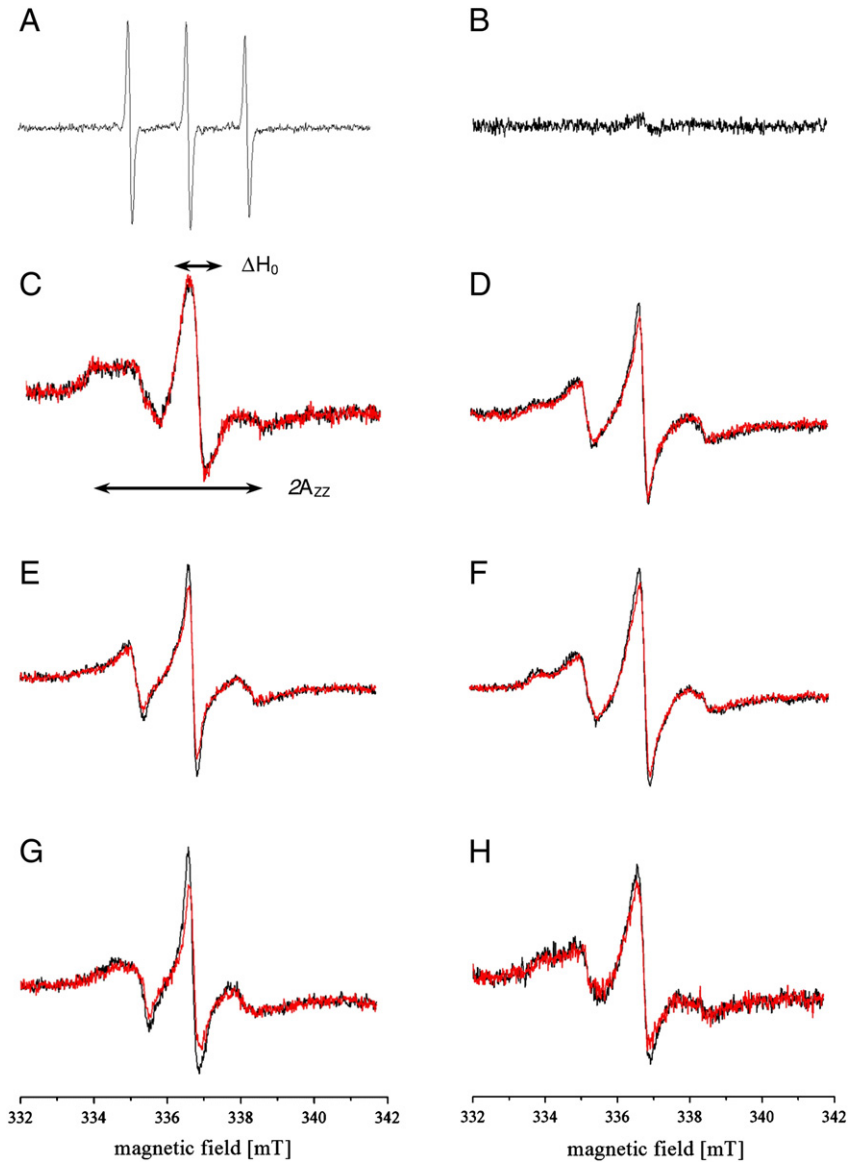

Fig. 3. EPR spectra of MTSL and MTSL bound to various complex I variants (4.5 mg/mL). (A) shows the spectrum of unbound MTSL in the same buffer containing lipids as used for the samples with protein. (B) shows the spectrum of *E. coli* wild type, (C) the variant R112C^{NuoB}, (D) the variant E84C^{NuoG}, (E) the variant E156C^{NuoE}, (F) the variant E298C^{NuoG}, (G) the variant D56C^{NuoF}, and (H) the variant T166C^{NuoM} either with (red) or without (black) an addition of 150 μM NADH. Minor differences between the spectra of the oxidized and reduced samples are due to slightly different protein concentrations and can be eliminated by multiplying the spectrum of the reduced sample with the dilution factor. The EPR conditions were the following: room temperature, microwave frequency: 9.458 GHz, microwave power: 10 mW, modulation amplitude: 0.2 mT, modulation frequency: 100 kHz, time constant: 82 ms, scan rate: 7.2 mT/min. Ten spectra of 10 μL sample were recorded for each curve.

movement of the secondary structure element containing the bound label relative to the entire protein [30]. Due to its large size, the overall rotation of the protein is slow, and thus the influence of τ_R on the shape of the EPR signal is negligible, leaving the rotation of the label relative to the protein and the movement of the secondary structure elements as determining factors for motional EPR line narrowing of an inhomogeneously broadened signal. To estimate the contribution of the effective correlation time τ_S to the line shape of the EPR signal, the mean *B*-factors at the corresponding positions were calculated from the published structure (Table 2) [39].

In the peripheral arm, each cysteine residue was introduced into an α-helix; thus, a similar mobility of the secondary structure element was expected. This holds true for the positions R112C^{NuoB}, E156C^{NuoE}, and D56C^{NuoF} (Table 2). Only small restrictions in the label mobility were detected for the positions E156C^{NuoE} and D56C^{NuoF} (Fig. 3) indicating that there are only negligible restrictions to the rotation of the label or only minor tertiary interactions. In contrast, the small inverse linewidth of the central resonance line of the label attached to position R112C^{NuoB} is not in accordance with the rather large *B*-factor, thus indicating contacts with tertiary structure elements. In contrast to the other positions labeled, R112C^{NuoB} is partly buried in the protein (Fig. 1), which might explain the tertiary interactions. The

Table 2
Spectral properties of MTSL covalently bound to different positions of complex I and the mean *B*-factors of the main chain atoms of the labeled positions and the labeled secondary structure element, respectively, taken from the pdb file 2FUG.

MTSL bound to	ΔH_0^{-1} [mT^{-1}]	$2A_{zz}$ [mT]	Mean *B*-factor amino acid/α-helix [Å^2]
Free	12.50	2.10	–
R112C^{NuoB}	2.13	4.88	78.8/66.6
E156C^{NuoE}	6.44	3.47	72.6/67.4
D56C^{NuoF}	5.56	3.63	70.1/63.0
E84C^{NuoG}	5.46	4.62	69.4/45.0
E298C^{NuoG}	1.88	4.94	85.5/83.1
T166C^{NuoM}	2.24	4.82	–

restricted mobility at this position is not due to an interaction with lipids, as an identical spectrum was obtained with samples in buffer without lipids (data not shown). The backbone mobility of position E84C^{NuoG} is not clearly defined due to the considerable difference between the *B*-factor of the engineered position and the entire helix (Table 2). The nearly unrestricted mobility of the label is, however, indicative of high backbone mobility as well as of a complete lack of tertiary interactions (Fig. 3). The strongly confined mobility of the label at position E298C^{NuoG} as implicated from the EPR spectrum (Fig. 3) indicated the presence of strong tertiary contacts despite the enhanced mobility of the corresponding helix that is expected from the large *B*-factor (Table 3). The EPR spectrum of the T166C^{NuoM} variant indicates interactions with neighboring residues or structural elements (Table 2).

An addition of 150 μM NADH to the samples did not significantly change the EPR spectra (Fig. 3) indicating that neither the binding of NADH nor the reduction of the complex led to a change in the mobility of the label at the indicated positions. This was expected due to the more or less undisturbed mobility of the label bound to E156C^{NuoE}, D56C^{NuoF}, and E84C^{NuoG}. Since the restrictions of the label movement bound to R112C^{NuoB}, E298C^{NuoG} and T166C^{NuoM} did not change upon an addition of NADH, the environment of the corresponding α-helices on NuoB and NuoG as well as the loop region S162 to K173 on NuoM remained unaffected due to conformational rearrangements upon an addition of NADH. These data indicate that an addition of NADH does not lead to significant changes of the environment of the positions that have been labeled with MTSL. This is an unexpected finding since it was proposed that NADH binding leads to conformational changes all over the peripheral arm [21,22,42].

No interactions were detectable between the Fe/S clusters of complex I and the MTSL label covalently attached to the surface of complex I in the experiments described above. This was expected for several reasons. Firstly, the distances between the Fe/S clusters and the MTSL label are too large to allow an interaction between the spins. The shortest distance of 22 Å is found between N2 and position R112C^{NuoB}. It was reported that the largest distance at which interactions in a continuous waves (cw)-EPR experiment can be detected is 20 Å [35]. Secondly, the spectra were recorded at room temperature, at which the Fe/S clusters relax so fast so that the dipolar interactions escape detection by cw-EPR spectroscopy.

5. Synthesis and characterization of Q_{10}-MTSL

To determine the position of the ubiquinone binding site a quinone analog was synthesized with an MTSL group attached at the C10 position of the decyl chain of decyl-ubiquinone. It is known that substitutions of the headgroup of quinones are sensitive binding determinants [43]. Therefore, not the headgroup but the side chain was chosen for modification with the spin label. The first three isoprene units of the side chain are needed for a tight binding of the quinone [44,45]. Thus, it is expected that the ten carbon atoms of the alkyl side chain of decyl-ubiquinone and the MTSL spin label are tightly bound to complex I and will occupy a distinct and physiologically meaningful position. The detailed procedure for its synthesis will be published elsewhere. In principle, an addition of di-(11-bromo-undecanoyl)-peroxide to 2,3 dimethoxy-5-methyl-1,4-benzoquinone gave 6-(10-bromodecyl)-ubiquinone. Potassium thioacetate was added to the purified bromodecyl-ubiquinone to obtain 6-(10-S-acetyldecyl)-ubiquinone. Addition of MTSL led to the formation of Q_{10}-MTSL (Fig. 4).

Q_{10}-MTSL was identified by means of mass spectrometry ($Mass_{theor.}$: 539, $Mass_{exp.}$: 539) as well as by UV/vis spectroscopy and its structure confirmed by NMR spectroscopy (data not shown). The attachment of the nitroxide label to the quinone was demonstrated by EPR spectroscopy (Fig. 4). Interactions between the Fe/S clusters of complex I and the MTSL label covalently attached either to the quinone or to the protein were not expected, because during the experiment the clusters are in an oxidized state and thus, diamagnetic. Performing the EPR measurement at 40 K suppresses the mobility of the spin label, thus excluding other influences that might interfere with the distance measurements. In addition to the para-quinone moiety, Q_{10}-MTSL contains the possibly redox active nitroxide group at the pyrroline moiety, which might interfere with the redox reaction of complex I. To examine this possibility, the midpoint potential of the redox active groups of the synthesized Q_{10}-MTSL was determined by means of cyclovoltammetry in H_2O/ethanol (5:1). A single peak at a potential of + 196 mV (vs. NHE at pH 8.0) was detected. The redox reaction was coupled to protonation reactions as expected for the quinone moiety. No other peak was detected in the range from −1 V to + 1V indicating that the midpoint potential of the nitroxide group is outside the physiological range and therefore not expected to interfere with the redox reaction of complex I.

To test whether Q_{10}-MTSL is a substrate for the *E. coli* complex I, the physiological NADH:ubiquinone oxidoreductase activity was measured. In the presence of 150 μM NADH and 60 μM decyl-ubiquinone or Q_{10}-MTSL, respectively, an activity of 2.3 μmol min^{-1} mg^{-1} and 0.5 μmol min^{-1} mg^{-1} was obtained. Thus, the activity with the modified quinone was approximately one fifth compared to the activity using decyl-ubiquinone. However, the Q_{10}-MTSL was bound to the physiological ubiquinone reduction site, because both activities were inhibited by more than 95% upon the addition of piericidin A.

Table 3
EPR parameters of Q_{10}-MTSL and Q_{10}-MTSL bound to the complex I variant R112C^{NuoB}-MTSL obtained by simulations of the spectra shown in Fig. 4.

Sample		*g*-tensor[1]	*A*-tensor [MHz][2]	Spin–spin interaction [MHz][3]	Distance [Å][4]
Q_{10}-MTSL		2.0073	6.0	n.a.	n.a.
		2.0032	11.0		
		2.0007	96.1		
Q_{10}-MTSL + complex I R112C^{NuoB}-MTSL	MTSL 1	2.0064	4.9	−50.0	13.5 ± 1.5 Å
		2.0051	4.8	−40.0	
		2.0033	96.6	−40.4	
	MTSL 2	2.0087	24.3		
		2.0071	24.8		
		2.0014	96.5		

[1] The standard deviation was ± 0.0005.
[2] The standard deviation was ± 2.0 MHz.
[3] The standard deviation was ± 2.0 MHz.
[4] Distances were calculated using the spin–spin interaction of the EasySpin simulation. The exchange interaction *J* (with its exponential distance dependence $J(r) = J_c e^{-3r}$) was ignored in the calculations as *J* only contributes significantly at distances below 1.0 nm. Thus, the distance dependence of the spin–spin interaction was calculated via the point-dipol approximation ($D(r) = 2.87 \times 10^3/r^3$).

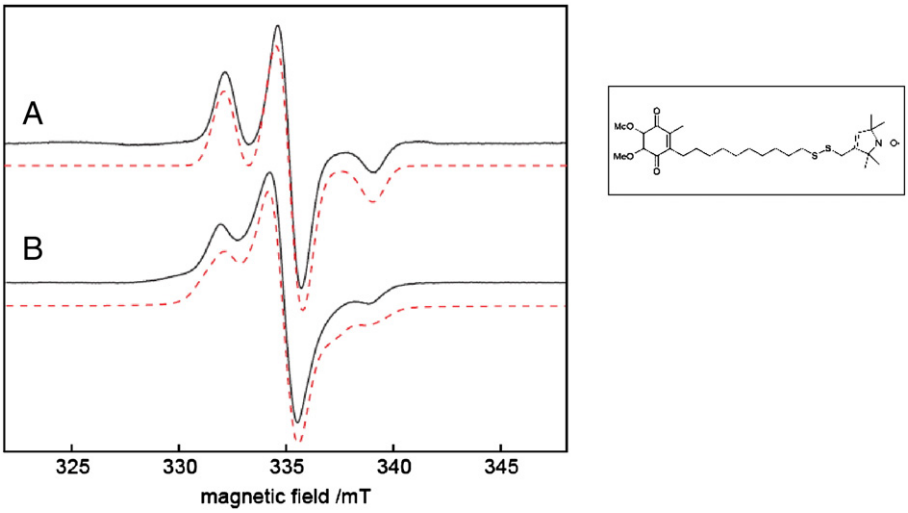

Fig. 4. EPR spectra of free and protein bound Q_{10}-MTSL. (A) Q_{10}-MTSL in solution. (B) Q_{10}-MTSL bound to MTSL-labeled complex I R112C^{NuoB}. Spectral simulations are shown as red dashed lines. The inset shows the structure of Q_{10}-MTSL. Experimental parameters: microwave frequency: 9.363 GHz, microwave power: 2 mW, modulation amplitude: 0.3 mT, modulation frequency: 100 kHz, and temperature: 40 K.

6. EPR spectroscopy of Q_{10}-MTSL bound to MTSL-labeled complex I

The distance between the MTSL bound to position R112C^{NuoB} of complex I and the MTSL bound to the quinone was determined by quantification of their mutual spin–spin interaction comprising an exchange and a dipolar contribution. Both are modulated by residual motion of the spin label side chains. The static dipolar interaction in an unordered, immobilized sample leads to considerable broadening of the cw-EPR spectrum if the interspin distance is less than about 20 Å [46].

Interspin distances were extracted from cw-EPR spectra of frozen protein samples via simulation [47]. For this purpose, Q_{10}-MTSL was added in an equimolar ratio to the labeled complex I and cw-EPR spectra were recorded at X-Band microwave frequencies at 40 K. For comparison, a cw-EPR spectrum of Q_{10}-MTSL in solution was recorded (Fig. 4A). By mere inspection of the two EPR spectra it is evident that the spectrum containing Q_{10}-MTSL bound to spin-labeled complex I is clearly broadened and shows distinct changes in its hyperfine splitting when compared to the spectrum of Q_{10}-MTSL in solution.

Spectral simulations were performed using a self-written Matlab (The MathWorks, Natick, MA) routine based on the EasySpin package [48]. Two *g* and *A* tensors for the two interacting MTSL radicals, and electron-electron interaction parameters were adjusted to obtain the best possible agreement of simulated and experimental spectra (Fig. 4A and B, dotted lines). The best-fit *g* and *A* values for the two EPR spectra are summarized in Table 3. An isotropic electron-electron interaction tensor of 25 MHz, corresponding to a distance of 13.5 ± 1.5 Å, was obtained. The error derives mainly from the poorly resolved MTSL spectra recorded at X-Band frequencies. However, at present we cannot exclude that in addition to spin–spin interaction, a distance distribution between the two paramagnetic centers also significantly contributes to spectral broadening. The 13.5 Å distance between the two labels is too short to use pulsed EPR techniques for distance determination [35]. Currently, we are generating new mutants with cysteine residues at positions suitable for pulsed EPR techniques.

Recently, the structure of the entire complex I from *T. thermophilus* was determined at 4.5 Å and the structure of the membrane arm of the *E. coli* complex I at 3.9 Å resolution [49]. Although the structure does not show the presence of bound quinone, it was proposed that a large cavity at the interface between NuoB and NuoCD binds the hydrophilic quinone head group [49]. This proposal is supported by the position of the cavity at the distal end of the electron transfer chain provided by Fe/S clusters, by labeling of the domain with inhibitors of the quinone-binding site, and by data obtained by site-directed mutagenesis [20,49]. However, the structure does not give any hints on the conformation of the hydrophobic isoprenoid chain of bound quinone. Thus, the exact distance between the label attached to R112C^{NuoB} and that attached to the C10 position of the decyl chain of decyl-ubiquinone cannot be derived from the structure. Nevertheless, the distance of 13.5 Å between the two labels is in agreement with the proposed localization of the quinone binding site in complex I. Positioning a decyl-ubiquinone molecule in the proposed binding pocket results in a kinked conformation of the isoprenoid chain when taking the measured distance into account.

Our data clearly demonstrate that Q_{10}-MTSL binds at a defined position to the MTSL-labeled complex I. In addition, they show that by binding Q_{10}-MTSL to MTSL-labeled complex I and by exploiting the mutual spin–spin interaction between the labels using EPR, geometric information on complex I is obtained. Combining a geometric examination of the suggested binding site and our distance data, a location of the quinone head group within a distance of 15 Å to the terminal cluster N2 is likely. Ideally, additional EPR experiments, particularly exploiting the advantages of high-field (and pulsed) EPR, have yet to be performed to improve our distance calculations.

7. Outlook

Altogether, we have established a system that allows the nitroxide spin label MTSL to decorate complex I at distinct positions, and we have synthesized a substrate of the complex that binds to its physiological ubiquinone binding site and that is modified by the same label. The distance calculated between the quinone and the complex I position labeled with MTSL is in agreement with the proposed position of the quinone binding site [49]. Using additional complex I variants and pulsed electron–electron double resonance, we are aiming to determine the exact orientation of the ubiquinone in its binding site in complex I by a triangulation strategy.

Acknowledgments

This work was supported by the Deutsche Forschungsgemeinschaft (DFG) by a grant to TF and by the Agence National de Recherche (ANR) by a grant to PH. We thank Dr. Jürgen Wörth for mass spectrometry experiments and Linda Williams for her help in correcting the manuscript, and Prof. Dr. Heinz-Jürgen Steinhoff and Dr. Johann Klare for providing us with a simulation program for cw-EPR spectra.

References

[1] H. Weiss, T. Friedrich, G. Hofhaus, D. Preis, The respiratory-chain NADH dehydrogenase (complex I) of mitochondria, Eur. J. Biochem. 197 (1991) 563–576.
[2] J.E. Walker, The NADH:ubiquinone oxidoreductase (complex I) of respiratory chains, Q. Rev. Biophys. 25 (1992) 253–324.
[3] U. Brandt, Energy converting NADH:quinone oxidoreductase, Annu. Rev. Biochem. 75 (2006) 69–92.
[4] T. Friedrich, Complex I: a chimaera of a redox and conformation-driven proton pump? J. Bioenerg. Biomembr. 33 (2001) 169–177.
[5] T. Friedrich, T. Pohl, NADH as Donor (13 August 2007, posting date) Chapter 3.2.4, in: A. Böck, R. Curtiss III, J.B. Kaper, F.C. Neidhardt, T. Nyström, J.M. Slauch, C.L. Squires (Eds.), EcoSal—*Escherichia coli* and *Salmonella:* cellular and molecular biology, ASM Press, Washington, DC, 2007http://www.ecosal.org.
[6] T. Yagi, A. Matsuno-Yagi, The proton-translocating NADH-quinone oxidoreductase in the respiratory chain: the secret unlocked, Biochemistry 42 (2003) 2266–2274.
[7] T. Ohnishi, J.C. Salerno, Conformation-driven and semiquinone-gated proton-pump mechanism in the NADH-ubiquinone oxidoreductase (complex I), FEBS Lett. 579 (2005) 4555–4561.
[8] L.A. Sazanov, Respiratory complex I: mechanistic and structural insights provided by the crystal structure of the hydrophilic domain, Biochemistry 46 (2007) 2275–2288.
[9] T. Friedrich, K. Steinmüller, H. Weiss, The proton-pumping respiratory complex I of bacteria and mitochondria and its homologue in chloroplasts, FEBS Lett. 367 (1995) 107–111.
[10] T. Friedrich, The NADH:ubiquinone oxidoreductase (complex I) from *Escherichia coli*, Biochim. Biophys. Acta 1364 (1998) 134–146.
[11] V. Spehr, A. Schlitt, D. Scheide, V. Guenebaut, T. Friedrich, Overexpression of the *Escherichia coli* nuo-operon and isolation of the overproduced NADH:ubiquinone oxidoreductase (complex I), Biochemistry 38 (1999) 16261–16267.
[12] V. Guénebaut, A. Schlitt, H. Weiss, K.R. Leonard, T. Friedrich, Consistent Structure Between Bacterial and Mitochondrial NADH:Ubiquinone Oxidoreductase (Complex I), J. Mol. Biol. 276 (1998) 105–112.
[13] N. Grigorieff, Structure of the respiratory NADH:ubiquinone oxidoreductase (complex I), Curr. Opin. Struct. Biol. 9 (1999) 476–483.
[14] T. Friedrich, B. Bottcher, The gross structure of the respiratory complex I: a Lego System, Biochim. Biophys. Acta 1608 (2004) 1–9.
[15] E.A. Baranova, P.J. Holt, L.A. Sazanov, Projection structure of the membrane domain of *Escherichia coli* respiratory complex I at 8 A resolution, J. Mol. Biol. 366 (2007) 140–154.
[16] T. Clason, T. Ruiz, H. Schägger, G. Peng, V. Zickermann, U. Brandt, H. Michel, M.M. Radermacher, The structure of eukaryotic and eukaryotic complex I, J. Struct. Biol. 169 (2010) 81–88.
[17] E. Nakamaru-Ogiso, A. Matsuno-Yagi, S. Yoshikawa, T. Yagi, T. Ohnishi, Iron-sulfur cluster N5 is coordinated by an HXXXCXXCXXXXXC motif in the NuoG subunit of *Escherichia coli* NADH:quinone oxidoreductase (complex I), J. Biol. Chem. 283 (2008) 25979–25987.
[18] G. Yakovlev, T. Reda, J. Hirst, Reevaluating the relationship between EPR spectra and enzyme structure for the iron sulfur clusters in NADH:quinone oxidoreductase, Proc. Natl Acad. Sci. USA 104 (2007) 12720–12725.
[19] I. Prieur, J. Lunardi, A. Dupuis, Evidence for a quinone binding site close to the interface between NuoD and NuoB subunits of complex I, Biochim. Biophys. Acta 1504 (2001) 173–178.
[20] U. Fendel, M.A. Tocilescu, S. Kerscher, U. Brandt, Exploring the inhibitor binding pocket of respiratory complex I, Biochim. Biophys. Acta 1777 (2008) 660–665.
[21] A.A. Mamedova, P.J. Holt, J. Carroll, L.A. Sazanov, Substrate-induced conformational change in bacterial complex I, J. Biol. Chem. 279 (2004) 23830–23836.
[22] T. Pohl, D. Schneider, R. Hielscher, S. Stolpe, K. Dörner, M. Kohlstädt, B. Böttcher, P. Hellwig, T. Friedrich, Nucleotide-induced conformational changes in the *Escherichia coli* NADH:ubiquinone oxidoreductase (complex I), Biochem. Soc. Trans. 36 (2008) 971–975.
[23] P. Hellwig, S. Stolpe, T. Friedrich, T., FTIR spectroscopic study on the conformational reorganization in *E. coli* complex I due to redox-driven proton translocation, Biopolymers 74 (2004) 69–72.
[24] P. Hellwig, D. Scheide, S. Bungert, W. Mäntele, T. Friedrich, FT-IR spectroscopic characterization of NADH:ubiquinone oxidoreductase (complex I) from *Escherichia coli*: Oxidation of FeS cluster N2 is coupled with the protonation of an Aspartate or Glutamate side chain, Biochemistry 39 (2000) 10884–10891.
[25] G.I. Belogrudov, Y. Hatefi, Catalytic sector of complex I (NADH:ubiquinone oxidoreductase): subunit stoichiometry and substrate-induced conformation changes, Biochemistry 33 (1994) 4571–4576.
[26] S.D. Patel, C.I. Ragan, Structural studies on mitochondrial NADH dehydrogenase using chemical cross-linking, Biochem. J. 256 (1988) 521–528.
[27] W.L. Hubbell, C. Altenbach, Investigation of structure and dynamics in membrane proteins using site-directed spin labeling, Curr. Opin. Struct. Biol. 4 (1994) 566–573.
[28] L.J. Berliner, J. Grunwald, H.O. Hankovszky, K. Hideg, A novel reversible thiol-specific spin label: papain active site labeling and inhibition, Anal. Biochem. 119 (1982) 450–455.
[29] A. Columbus, W.L. Hubbell, A new spin on protein dynamics, Trends Biochem. Sci. 27 (2002) 288–295.
[30] H.S. Mchaourab, M.A. Lietzow, K. Hideg, W.L. Hubbell, Motion of spin-labeled side chains in T4 lysozyme. Correlation with protein structure and dynamics, Biochemistry 35 (1996) 7692–7704.
[31] S. Mehboob, B.H. Luo, W. Fu, M.E. Johnson, L.M.W. Fung, Conformational studies of the tetramerization site of human erythroid spectrin by cystein-scanning spin-labeling EPR methods, Biochemistry 44 (2005) 15898–15905.
[32] M. Pfeiffer, T. Rink, K. Gerwert, D. Oesterhelt, J.H. Steinhoff, Site-directed spin labeling reveals the orientation of the amino acid side-chains in the E-F loop of bacteriorhodopsin, J. Mol. Biol. 287 (1999) 163–171.
[33] W.L. Hubbell, H.S. Mchaourab, C. Altenbach, M.A. Lietzow, Watching proteins move using site-directed spin labeling, Structure 4 (1996) 779–783.
[34] J. Steinhoff, Inter- and intra-molecular distances determined by EPR spectroscopy and site-directed spin labeling reveal protein-protein and protein-oligonucleotide interaction, Biol. Chem. 385 (2004) 913–920.
[35] E.J. Hustedt, A.I. Smirnov, F.L. Laub, C.E. Cobb, A.H. Beth, Molecular distances from dipolar coupled spin-labels: the global analysis of multifrequency CW-EPR data, Biophys. J. 74 (1997) 1861–1877.
[36] G. Jeschke, Distance measurements in the nanometer range by pulse EPR, Chemphyschem 3 (2002) 927–932.
[37] A. Schweiger, G. Jeschke, Principles of Pulse Electron Paramagnetic Resonance, OUP, Oxford, 2001.
[38] T. Pohl, M. Uhlmann, M. Kaufenstein, T. Friedrich, Lambda Red-mediated mutagenesis and efficient large scale affinity purification of the *Escherichia coli* NADH:ubiquinone oxidoreductase (complex I), Biochemistry 46 (2007) 10694–10702.
[39] L.A. Sazanov, P. Hinchliffe, Structure of the hydrophilic domain of respiratory complex I from *Thermus thermophilus*, Science 311 (2006) 1430–1436.
[40] J. Nielson, B. Persson, G.von Heijne, Consensus predictions of membrane protein topology, FEBS Lett. 486 (2000) 267–269.
[41] A. Czogalla, A. Pieciul, A. Jezierski, A.F. Sikorski, Attaching a spin to a protein – site-directed spin labeling in structural biology, Acta Biochim. Polon. 54 (2007) 235–244.
[42] N. Hano, Y. Nakashima, K. Shinzawa-Itoh, S. Yoshikawa, Effect of the side chain structure of coenzyme Q on the steady state kinetics of bovine heart NADH: coenzyme Q oxidoreductase, J. Bioenerg. Biomembr. 35 (2003) 257–265.
[43] J.C. McComb, R.R. Stein, C.A. Wraight, Investigations on the influence of headgroup substitution and isoprene side-chain length in the function of primary and secondary quinones of bacterial reactions centers, Biochim. Biophys. Acta 1015 (1990) 156–171.
[44] G. Hauska, E. Hurt, Pool Function Behaviour and Mobility of Isoprenoid Quinones, in: B.L. Trumpower (Ed.), Function of Quinones in Energy Conserving Systems, Academic Press, New York, 1982, pp. 87–110.
[45] A. Baccarini-Melandri, N. Gabellini, B.A. Melandri, E. Hurt, G. Hauska, Structural requirements of quinone coenzymes for endogenous and dye-mediated coupled electron transport in bacterial photosynthesis, J. Bioenerget. Biomembr. 12 (1980) 95–110.
[46] J.P. Klare, H.J. Steinhoff, Spin labeling EPR, Photosynth. Res. 102 (2009) 377–390.
[47] H.J. Steinhoff, N. Radzwill, W. Thevis, V. Lenz, D. Brandenburg, A. Antson, G. Dodson, A.Wollmer, Determination of interspin distances between spin labels attached to insulin: comparison of electron paramagnetic resonance data with the X-ray structure, Biophys. J. 73 (1997) 3287–3298.
[48] S. Stoll, A. Schweiger, EasySpin, a comprehensive software package for spectral simulation and analysis in EPR, J. Magn. Reson. 178 (2006) 42–55.
[49] R.G. Efremov, R. Baradaran, L.A. Sazanov, The architecture of respiratory complex I, Nature 465 (2010) 441–447.